Experimental Hamiltonian Identification for Qubits subject to Multiple Independent Control Mechanisms.

Sonia G. Schirmer*, Avinash Kolli*, Daniel K. L. Oi* and Jared H. Cole†

*Dept of Applied Maths and Theoretical Physics, University of Cambridge, Wilberforce Rd, Cambridge, CB3 0WA, United Kingdom
†Centre for Quantum Computer Technology, School of Physics, University of Melbourne, Melbourne, Australia

Abstract. We consider a qubit subject to various independent control mechanisms and present a general strategy to identify both the internal Hamiltonian and the interaction Hamiltonian for each control mechanism, relying only on a single, fixed readout process such as $\hat{\sigma}_z$ measurements.

1. INTRODUCTION

Realizing the ultimate goal of quantum information processing, namely building a working quantum computer, is to a large extent a problem of finding ways to control the dynamics of a quantum system precisely. A crucial prerequisite for this task is one's ability to accurately determine of the dynamics of the physical system and its response to external (control) fields. Quantum process tomography (QPT), by providing a general procedure to identify the unitary (or completely positive) processes acting on a system, addresses this problem but does not solve it completely.

One problematic aspect of QPT is the assumption that one can experimentally determine the expectation values of a complete set of observables, or at least perform *arbitrary* single qubit measurements on a register of n qubits. Most QIP proposals rely on a single readout process, i.e., measurement in a fixed basis. For example, qubits encoded in internal electronic states of trapped ions or neutral atoms are read out by quantum jump detection via a cycling transition; readout for solid-state qubits based on Cooper-pair boxes, Josephson junctions, or electrons in double-well potentials usually involves charge localization using single electron transistors or similar devices. Finally, solid state architectures based on electron or nuclear spin qubits are expected to be limited to σ_z measurements via spin-charge transfer.

It is usually assumed that local projective measurements in a fixed basis are sufficient since arbitrary single qubit measurements can then be realized by performing a local unitary transformation before measuring to achieve a change of basis. However, implementing such a basis change requires precise knowledge of the dynamics of each individual qubit and its response to control fields in the first place, the very information we seek to determine experimentally, and which may be difficult to *predict* precisely based on theoretical models and computer simulations alone, in particular for systems that are sensitive to fabrication variance. A possible solution to this seemingly intractable problem was described in [1]. In the following we outline the general strategy, discuss various ways of extracting the system parameters from noisy experimental data, and illustrate the key steps using examples with simulated measurement data.

2. GENERAL STRATEGY FOR HAMILTONIAN IDENTIFICATION

The state of a two-level system can be mapped to a Bloch vector $\mathbf{s}$, i.e., a real vector in $\mathbb{R}^3$, with pure states corresponding to points on the Bloch sphere, i.e., the surface of the unit ball. On timescales sufficiently short compared to the decoherence time, the evolution of the system is governed by a Hamiltonian, which can be written in terms of the Pauli matrices $\hat{\sigma}_*$ for $* \in \{x,y,z\}$, $2\hat{H} = d_0\hat{I} + d_x\hat{\sigma}_x + d_y\hat{\sigma}_y + d_z\hat{\sigma}_z$, where d_0, d_x, d_y and d_z are real constants. If the Hamiltonian remains constant for $t_0 \le t \le t_1$, the Bloch vector undergoes a rotation about the axis $\mathbf{d} = (d_x, d_y, d_z)$.

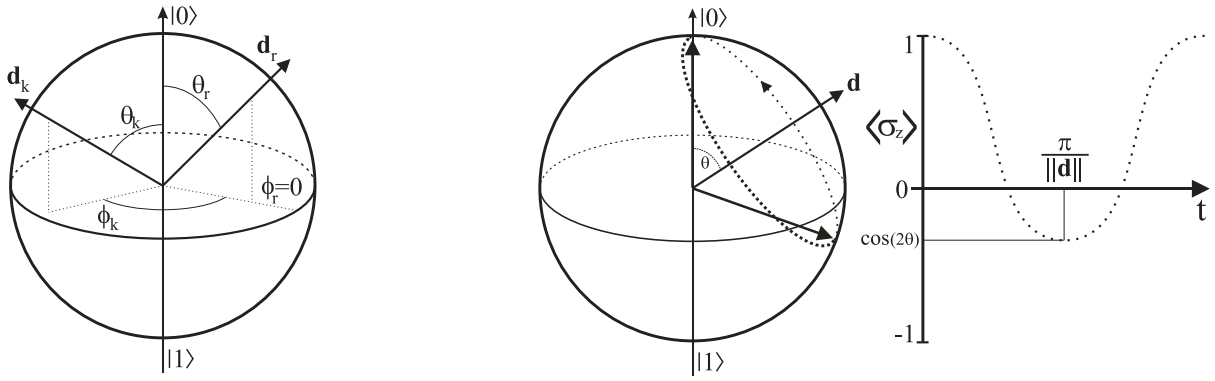

FIGURE 1. Left: Declinations θ and relative azimuthal angles ϕ for two rotation axes. Right: Determination of the rotation frequency and angle θ of the rotation axis by mapping the precession of the state $|0\rangle$.

The length $||\mathbf{d}||$ of this vector determines rotation frequency; the rotation axis can be specified by a unit vector $\hat{\mathbf{d}} = (\sin\theta\cos\phi, \sin\theta\sin\phi, \cos\theta)^T$, i.e., by two angles θ and ϕ as shown in Fig. 1. To identify the parameters d_x, d_y and d_z of the Hamiltonian it therefore suffices to determine the rotation frequency and the angles θ and ϕ. Since d_0 results only in an unobservable global phase factor, it can be ignored.

If the system can be repeatedly initialized in a known state, e.g., one of the measurement basis states $|0\rangle$ or $|1\rangle$, and then measured after having evolved for progressively longer time periods, we can map the trajectory of the z-component of the Bloch vector, and extract the frequency and angle θ of the rotation as shown in Fig. 1 (right). For some systems such as NMR-based schemes this may be sufficient as the phase relationship between d_x and d_y is fixed by the phase relationship between the control fields. In general, however, a second series of measurements is necessary to determine the horizontal angle ϕ of the rotation axis with respect to a reference axis $\mathbf{d}_r$. This procedure is given in Ref. [1] and involves using the values of θ and $||\mathbf{d}||$ determined in the first step to select a different initial state, and mapping its precession about the desired rotation axis.

For a system subject to various control fields f_m (e.g., fields associated with different control electrodes) in addition to its free evolution, we must determine both its internal Hamiltonian $\hat{H}_0$ and the interaction Hamiltonian $\hat{H}_m$ for each independent control mechanism. Although we usually cannot determine the interaction Hamiltonians directly since we cannot switch off the internal dynamics, we can identify the rotation axis $\mathbf{d}_{0+m}^{(k)} = \mathbf{d}_0 + f_m^{(k)}\mathbf{d}_m$ corresponding to the evolution of the system under the Hamiltonian $\hat{H}_0 + f_m^{(k)}\hat{H}_m$ for a fixed control setting $f_m = f_m^{(k)}$. Repeating this procedure for each available control field f_m with several control field settings $f_m^{(k)}$ then allows us to extract both the internal and interaction parts of the Hamiltonian provided that the dependence of the Hamiltonian on the control fields is linear. (Nonlinear field effects require additional correction terms, and we will exclude this case in this paper.)

3. MAPPING $z(t)$ AND EXTRACTING THE RELEVANT DATA

A crucial factor in the Hamiltonian identification strategy outlined above is the mapping of the evolution of $z(t)$ as the system precesses around a fixed rotation axis. The accuracy with which we can identify the relevant parameters such as the rotation frequency and angle θ depends on the total length of time t_f for which $z(t)$ is mapped, the time resolution Δt and the uncertainty of each data point $z(t_k) = \langle\sigma_z(t_k)\rangle$, which depends on the number of times N_e each experiment is repeated to obtain the ensemble average (in addition to the frequency of measurement errors etc). The total number of measurements required to map $z(t)$ is thus $N_T = N_e t_f/\Delta t$. The choice of Δt, t_f and N_e will depend both on the system to be characterized and the method of data extraction to be used.

One possible approach is to use a small time step Δt and a large number of repetitions N_e to obtain a dense set of accurate data points for a period of time covering at least one quarter of the rotation period, and fit a cosine segment to the data. Since the time we have to monitor the evolution of $z(t)$ is limited by the decoherence time of the system, this approach may be useful for systems that decohere rapidly because it requires only sampling over a short period of time.

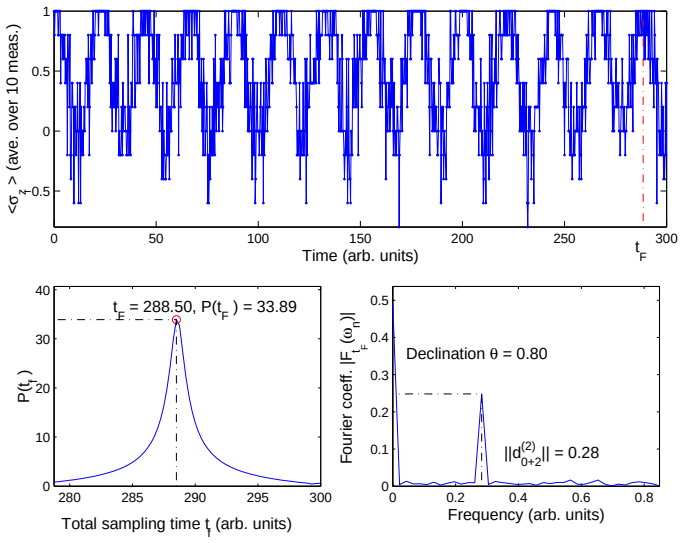

Figure 2: The top graph to the left shows an example of noisy (simulated) measurement data for rotations about $\mathbf{d}_0 + f_2^{(2)}\mathbf{d}_2$ with $f_2^{(2)} = 0.1$. The dash-dot line indicates the optimal sampling time t_F determined by finding the maximum of the function $P(t_f)$ (bottom-left). The Fourier transform of the (truncated) data for $0 \le t \le t_F$ is shown in the bottom-right graph. Its zero-frequency component determines $\theta = \arccos\sqrt{|F(0)|}$; and the location of the second peak gives the rotation frequency $\omega = ||\mathbf{d}_0 + f_2^{(2)}\mathbf{d}_2||$. The estimates obtained, $\theta = 0.80$ and $\omega = 0.28$, are close to the actual values $\theta = 0.7854$ and $\omega = 0.2828$.

Another approach, explained in detail in [1], is to use relatively coarse time sampling, with a moderate number of repetitions for each data point, over several rotation periods to obtain a rough estimate of the rotation frequency using the discrete Fourier transform, followed by a second step of acquiring more accurate additional data points in the region where the first minimum of $z(t)$ is expected based on the first estimate, and fitting a parabola to the new data to find the rotation frequency and declination of the rotation axis.

A third alternative [2] is to eliminate curve-fitting altogether and extract all the required information directly from the Fourier transform. This method is rather elegant and does not require the high time resolution Δt and measurement repetition rates N_e usually necessary for curve-fitting methods. All we need to avoid aliasing is that Δt be less than half the rotation period T. Ensuring that this condition is satisfied requires a rough a priori estimate of T but this should normally not be a problem. It also permits easy estimation of the accuracy of the parameters. However, since the frequency resolution $\Delta\omega = 2\pi/t_f$, we must be able to map the data for a least two complete cycles to be able to extract the rotation frequency, and more cycles will be required to obtain a clearly defined peak in the frequency spectrum. Hence, this method will be most suited to systems whose decoherence time is sufficiently long to allow mapping of the evolution of $z(t)$ over several cycles.

4. ILLUSTRATIVE EXAMPLE

To demonstrate the procedure, we choose a test system with $\mathbf{d}_0 = (0.2, 0, 0.1)^T$, $\mathbf{d}_1 = (1,1,0)^T$ and $\mathbf{d}_2 = (0,0,1)^T$. Fig. 2 illustrates how we identify the rotation frequencies and declination angles for $f_1 = 0$ and $f_2 = 0.1$ following the 3rd approach outlined in Sec. 3. We sample $z(t)$ over several rotation periods with an intermediate time step ($\Delta t = 0.25$) and a small number of repetitions ($N_e = 10$) for each measurement. We then obtain an estimate of the rotation frequency by taking the Fourier transform of the data and finding the frequency ω_p such that $|F(\omega_p)| = \max_{n>0}|F(\omega_n)|$, where $F(\omega_n)$ is the nth Fourier coefficient. Since the sampling period is usually not an integer multiple of the rotation period, the peak in the Fourier spectrum will tend to be unsharp, and our estimate inaccurate. To improve it, we compute the function $P(t_f) = [F_{t_f}(\omega_p) - F_{t_f}(\omega_{p-1}) - F_{t_f}(\omega_{p+1})]/[F_{t_f}(\omega_{p-1}) + F_{t_f}(\omega_{p+1})]$ where F_{t_f} is the Fourier transform of the truncated data for $0 \le t \le t_f$ and ω_p is the frequency where the first peak in the spectrum (excl. $F(0)$) occurs, $|F_{t_f}(\omega_p)| = \max_{n>0}|F_{t_f}(\omega_n)|$. $P(t_f)$ assumes a maximum when t_f is an integer multiple of the rotation period, thus allowing us to find the optimal sampling time t_F. Fig. 3 illustrates how we can find the horizontal angles ϕ, having identified the rotation frequencies and angles θ for all control settings, using a local curve fitting approach similar to the second strategy outlined in Sec. 3 and described in Ref. [1]. Finally, Fig. 4 shows how we can extract $\mathbf{d}_0$ and $\mathbf{d}_m$ by plotting the x, y and z-components of the rotation axes $\mathbf{d}_0 + f_m^{(k)}\mathbf{d}_m$ versus $f_m^{(k)}$ for $m = 1,2$ and fitting straight lines to the data.

Figure 3: The system is initialized in state $\mathbf{s}_1 = (\cos\beta, \sin\beta, 0)^T$ (here $\beta = -1.0446$) by rotating $\mathbf{s}_0 = (0,0,1)^T$ about the reference axis $\mathbf{d}_r$ (here $\mathbf{d}_0$) by a suitable angle ψ, and the precession of $\mathbf{s}_1$ about $\mathbf{d}_0 + f_1^{(1)}\mathbf{d}_1$, whose frequency and θ are already known, is mapped. Using a small number of data points (stars) we find the x-intercept of $z(t)$ (circle), which allows us to estimate the location of the extrema of $z(t)$. Additional data points (dots) are then acquired in these regions, and parabolas fitted to the data. The desired angle $\phi = -\beta - \arcsin(\gamma\cos\delta/\sin\theta_r)$, where $\gamma = (z_{max} - z_{min})/2$ and $\delta = \pi - (\alpha_{min} + \alpha_{max})/2$ are determined by the vertices of the parabolas, and the values β and θ_r (known from part 1). We obtain $\phi = 0.34$, which is close to the actual value $\phi = 0.3218$.

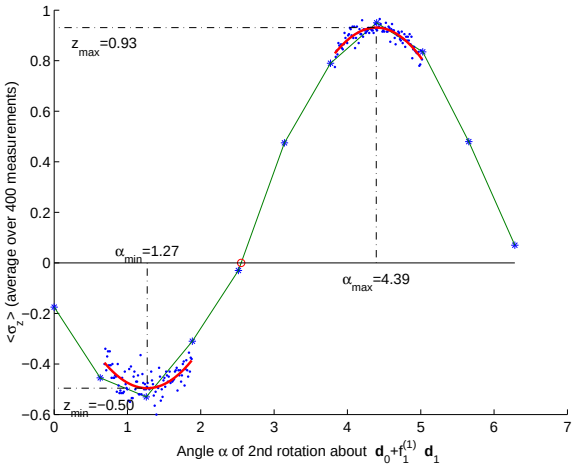

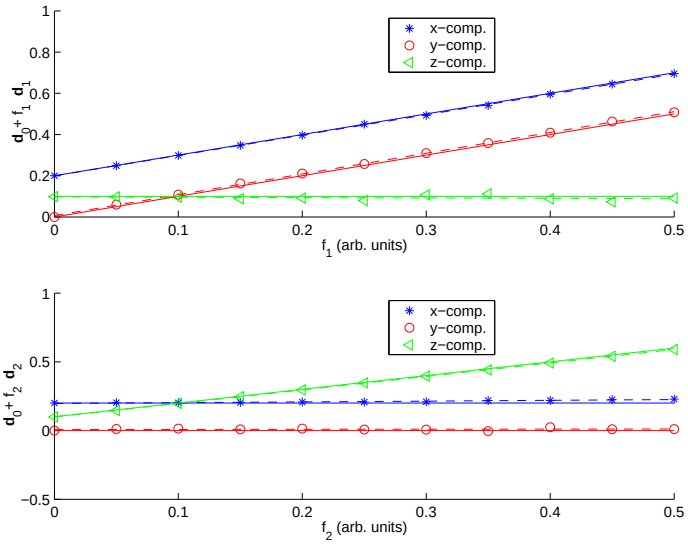

Figure 4: Having determined the rotation frequencies $\omega_{0+m}^{(k)}$ and the angles $\theta_{0+m}^{(k)}$ and $\phi_{0+m}^{(k)}$ of the rotation axes $\mathbf{d}_0 + f_m^{(k)}\mathbf{d}_m$ for various values of the controls f_1 and f_2, we convert the data into Cartesian coordinates, plot the values of the x, y and z-components of the axes $\mathbf{d}_0 + f_m^{(k)}\mathbf{d}_m$ for $m = 1,2$, respectively, and fit straight lines. The y-intercepts determine the x, y and z-components of $\mathbf{d}_0$, the slopes those of $\mathbf{d}_m$, for $m = 1,2$. For the data shown, we have

$$\begin{aligned} \mathbf{d}_0^{est} &= (0.1986, 0.0048, 0.0979)^T \\ \mathbf{d}_1^{est} &= (0.9884, 1.0163, 0.0087)^T \\ \mathbf{d}_2^{est} &= (0.0531, 0.0246, 0.9819)^T \end{aligned}$$

The distances $||\mathbf{d}_m^{est} - \mathbf{d}_m^{act}||$ of 0.0054, 0.0218 and 0.0613, respectively, compare favorably to the 3% readout error rate of the simulated experiments.

ACKNOWLEDGMENTS

We thank A. D. Greentree and L. C. H. Hollenberg for helpful discussions. S.G.S and D.K.L.O acknowledge financial support from the Cambridge-MIT Institute, Fujitsu, the UK goverment and IST grants RESQ (IST-2001-37559) and TOPQIP (IST-2001-39215). J.H.C acknowledges the support of the Australian Research Council, the Australian government, the US National Security Agency, The Advanced Research and Development Activity and the US Army Research Office (DAD19-01-1-0653). D.K.L.O also thanks Sidney Sussex College for support.

REFERENCES

1. Schirmer, S. G., Kolli, A., and Oi, D. K. L., *Phys. Rev. A*, **69**, 050603(R) (2004).
2. Cole, J. H., *et al.*, In preparation.